TOXICOLOGICAL SCIENCES **54,** 284–294 (2000)

Dermatotoxicokinetic Modeling of *p*-Nitrophenol and Its Conjugation Metabolite in Swine following Topical and Intravenous Administration

G. L. Qiao,*[,1] S. K. Chang,† J. D. Brooks,‡ and J. E. Riviere‡

**National Institute for Occupational Safety and Health (NIOSH), CDC, Morgantown, West Virginia 26505; †Department of Veterinary Medicine, National Taiwan University, Taipei, Taiwan, Republic of China; and ‡Center for Cutaneous Toxicology and Residue Pharmacology, North Carolina State University, Raleigh, North Carolina 27606*

Received September 3, 1999; accepted November 12, 1999

The development of a dermatotoxicokinetic (dTK) model for *p*-nitrophenol (PNP), a common metabolite from a variety of compounds and a biomarker of organophosphate (OP) insecticide exposure, may facilitate the kinetic modeling and risk assessment strategy for its parent compounds. In order to quantify and then clarify *in vivo-in vitro* correlation of PNP disposition, multicompartment kinetic models were formulated. Female weanling pigs were dosed with [^{14}C]PNP intravenously (150 μg in ethanol, n = 4) or topically onto non-occluded abdominal skin (300 μg/7.5cm^2 in ethanol, n = 4). PNP and *p*-nitrophenyl-β-D-glucuronide (PNP-G) profiles were determined in plasma and urine in addition to total ^{14}C quantitation in many other samples. Disposition parameters (rate constants, F_{top}, $T_{1/2}$, $T_{1/2Ka}$, AUC, Vss, C_{lp}, MAT, and MRT) and the simulated chemical mass-time profiles on the dosed skin surface and in the local, systemic, and excretory compartments were also determined. Total recoveries of 97.17 ± 4.18% and 99.80 ± 2.41% were obtained from topical and intravenous experiments, respectively. Ninety-six hours after topical and intravenous application, 70.92 ± 9.72% and 98.65 ± 2.43% of the dose were excreted via urine, and 0.55 ± 0.16% and 0.51 ± 0.10% via the fecal route, respectively. Peak excretion rate and time were also determined. It was suggested by experimental observation and modeling that urinary ^{14}C excretion correlates with the systemic tissue depletion profile well and may be used as a biomarker of PNP exposure. This study also supports the strategy of using urinary PNP as a biomonitoring tool for OP pesticide exposure, although some precautions have to be taken. The strategy used in this study will be useful in comprehensive dTK modeling in dermal risk assessment and transdermal drug delivery.

Key Words: p-nitrophenol (PNP); toxicokinetics; skin absorption; metabolism; pig.

The use of metabolic biomarkers to quantify systemic exposure to environmental chemicals receives increasing attention. Dermal exposure has been demonstrated to be a primary route for systemic exposure to many environmental chemicals (Honeycutt *et al.*, 1985; Wang *et al.*, 1989; Wester and Maibach, 1989). *p*-Nitrophenol (4-nitrophenol, PNP) is often used as a biomarker to quantitate dermal (Qiao *et al.*, 1994) or even oral exposure (Pena-Egido *et al.*, 1988) to many organophosphate (OP) pesticides such as parathion and methyl parathion. Although OP pesticide usage has been reduced in the United States since 1992, PNP dermal exposure hazard is still a concern due to PNP's direct use and its occupational or environmental appearance via pesticide degradation and waste disposal. Urinary excretion of PNP parallels urinary excretion of parathion and paraoxon after dermal parathion exposure in the pig (Qiao *et al.*, 1994). Additionally, a linear relationship exists between the plasma concentration of orally dosed parathion and the urinary excretion rate of PNP in the rabbit (Pena-Egido *et al.*, 1988). In order to use PNP as a biomarker for parent compound exposure, we should be prudent before an understanding of PNP's disposition after topical and systemic exposures independent of exposure to its parent pesticides can be established. Similarly, such an understanding is required to properly integrate *in vitro* dermal absorption data into *in vivo* risk assessment. This can best be accomplished by developing a comprehensive dermatotoxicokinetic (dTK) model of PNP disposition that can then be used to facilitate dTK modeling of its parent pesticides.

PNP is a common metabolite or degradation product of OP pesticides, occurring both *in vivo* in animals and humans and in the environment. According to a national survey, PNP is the fourth most commonly detected contaminant found in human urine screening in the United States (Kutz *et al.*, 1992). PNP is used mainly in the manufacture of drugs, fungicides, OP pesticides, and dyes, in addition to its direct use as a fungicide for leather products and as a leather-darkening agent. It can degrade in water and surface soil, but the breakdown takes longer in deeper soil and in groundwater. PNP has been detected in urine samples of people who did not have any known exposure to PNP. Of environmental concern, PNP often comes from the *in vivo* breakdown of common OP pesticides (e.g., parathion, methyl parathion) used in agriculture and forestry. PNP was selected as the sole biomarker used in a recent public health incident with methyl parathion house spray [Agency for Toxic

[1] To whom correspondence should be addressed at NIOSH, M/S 3030, 1095 Willowdale Rd., Morgantown, WV 26505–2888. Fax: (304) 285–6041. E-mail: gaq1@cdc.gov.

Substance And Disease Registry (ATSDR, 1996)]. However, due to PNP's coexposure potential with its parent compounds and PNP's dermal absorption-enhancing effect, proper usage of urine PNP as a biomarker for dermal exposure of OP pesticides and PNP (as a fungicide) requires careful kinetic evaluation of PNP dermatodisposition. Additionally, PNP has often served as a model substrate in conjugation studies with different *in vitro* and *in vivo* systems (Antoine *et al.*, 1993; Berry *et al.*, 1975; Bock *et al.*, 1973; Gessner, 1974; Hamada and Gessner, 1975; Machida *et al*., 1982; Minck *et al*., 1973; Moldeus *et al*., 1976; Vessey and Zakim, 1973; Vessey *et al.*, 1973) and has even been used in the purification of enzyme isoforms (Antoine *et al.*, 1993).

PNP can cause reversible blood disorders in both animals and humans, such as a decreased ability to carry O_2 to tissues (ATSDR, 1992) via methemoglobinemia, in addition to its CNS effects, mutagen activity, and direct burns on skin and eyes (Cooper *et al.*, 1997). Cutaneous irritation reactions such as erythema, edema, moderate to severe corneal cloudiness, blistered conjunctival tissue, and corneal neovascularization were observed in rats and rabbits after large-dose dermal exposure. Considerable ingestion of PNP also led to death of rats, mice, and rabbits. There is no evidence of carcinogenic activity in male and female Swiss-Webster mice receiving PNP topical doses of up to 160 mg/kg, three times/week for 78 weeks (ATSDR, 1992), although PNP is considered a mutagen (Cooper *et al.*, 1997).

The pig is a well-accepted animal model for studying human percutaneous absorption (Bartek *et al*., 1972; Hawkins and Reifenrath, 1984; Meyer *et al.*, 1978; Monteiro-Riviere and Riviere, 1996; Qiao *et al*., 1993; Reifenrath and Hawkins, 1986; Reifenrath *et al.*, 1984; Wester *et al.*, 1998). Topical absorption of PNP *in vitro* and *ex vivo* in porcine models have been examined (Brooks and Riviere, 1996; Chang *et al*., 1994a,b). Dermal absorption and dTK modeling were also conducted following intravenous (iv) and topical application of parathion, one of the PNP parent compounds (Qiao *et al.*, 1993; 1994; Qiao and Riviere, 1995). The parathion disposition dTK model included the parathion-derived PNP components, which provided a tool to explore the differences between the kinetic disposition of directly applied PNP and that of metabolically derived PNP in the *in vivo* porcine model. PNP disposition is relatively simple, as PNP is not significantly metabolized in the skin, and therefore the *in vivo* and *in vitro* disposition differences are minimized.

This study was designed to *a*) quantify the cutaneous and systemic disposition fate of PNP *in vivo* in swine by formulating a dTK model after iv and topical application; *b*) explore the similarity/difference of PNP disposition in the skin with direct topical PNP dose and with metabolically derived PNP; and *c*) facilitate the dTK modeling strategy for its parent compounds and in transdermal drug delivery and human dermal risk assessment studies.

MATERIALS AND METHODS

Animals

Eight- to ten-week-old female weanling Yorkshire pigs (~20 kg, T-Sharp, Rocky Mount, NC) were acclimated for 1 week. The animals were individually housed in metabolic cages (72°F and 12:12 h light:dark cycle), given 15% (protein) pig and sow pellets (~2 lbs/pig/day) and given free access to water. Eight pigs were randomly assigned to receive either topical or iv exposure (n = 4/exposure). Throughout the experiments, all pigs were humanely handled according to preapproved North Carolina State University animal use and care protocols.

Drugs and Chemicals

[^{14}C-ring-2,6]PNP (11.7 mCi/mmol) was purchased from Sigma Chemical Co. (St. Louis, MO). Ethanol (absolute, Aaper Alcohol and Chemical Co., Shelbyville, KY) was used as the dosing vehicle. Cold PNP (10 μg/μl) and *p*-nitrophenyl-β-D-glucuronide (PNP-G) (Sigma) were used in topical dose formulation and high performance liquid chromatography (HPLC) methodology development. Other chemicals were HPLC or gas chromatography (GC) grade.

Dosing

Topical application. Pigs were anesthetized with halothane following ketamine (11 mg/kg) + xylazine (1.5 mg/kg) intramuscular (im) injection. The ear vein and jugular veins were catheterized. Hair in the selected abdominal dosing site was clipped carefully 6 h prior to PNP dosing (Qiao *et al.*, 1993, 1997). Approximately 300 μg of PNP (150 μg cold PNP + 150 μg [^{14}C]PNP with 10 μCi total radioactivity) in 100 μl ethanol vehicle was evenly applied to a 7.5 cm^2 circular dosing zone in the abdominal area of pigs. This dose provided a surface concentration of 40 μg/cm^2. The dosed skin was non-occlusively protected by a Hill Top® chamber with holes, covered by nylon screening, and positioned by Elasticon® wrapping tape.

Intravenous dosing. To avoid any potential dose-dependent kinetics of PNP disposition in the pig, a smaller iv dosage (half of the total topical dose, i.e., 150 μg) was selected based on the estimated dermal PNP bioavailability of 50%. This pure labeled PNP (~10 μCi, no cold PNP) in ethanol was injected into the bloodstream through an ear vein cannula followed by a 10-ml physiologic saline flush to provide an instant and complete bolus dose.

Sampling and ^{14}C Assay

Blood samples (14 topical and 30 iv per animal, 5 ml each) were withdrawn via the jugular vein cannula from 0 to 96 h. Plasma was routinely separated. Urine was collected immediately after voiding. Feces samples were collected once a day, weighed, and homogenized with distilled water (~50:50, w/w). At 96 h postdosing, pigs were sacrificed and the dosing materials/devices were collected and extracted with ethyl acetate: Elasticon tape and screen 2 × 45 ml; dosing chamber 5 × 15 ml; cotton swabs for skin surface wash [10% dish-washing liquid (three times, Dove®, Lever Bros. Co., New York, NY) and water (three times)] 2 × 45 ml. The stratum corneum was isolated by tape stripping (10 times) and digested in ethyl acetate (15 ml per stripping). Full-thickness skin, subcutaneous fat, and muscle samples at the dosed site were carefully excised and assayed. All samples of tissues and excreta with detectable ^{14}C were also assayed for total ^{14}C recovery in our mass balance study. For more details, our original *in vivo* dermal absorption work should be consulted (Qiao *et al.*, 1993).

All the samples were stored at –20°C until analysis. An aliquot of 250–500 μl liquid or 100–700 mg solid sample was completely burned in a tissue oxidizer followed by Liquid Scintillation Counting (LSC, TriCarb 1900TR liquid scintillation analyzer, Packard Instrument Co., Downers Grove, IL) for total ^{14}C assay. HPLC separation was performed to study PNP metabolism as described below.

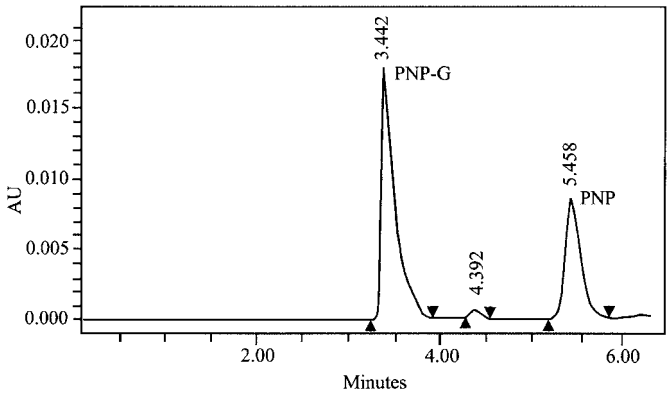

FIG. 1. Chromatogram of *p*-nitrophenol (PNP) and *p*-nitrophenyl-β-D-glucuronide (PNP-G): HPLC conditions: column = μ-Bondapack C_{18} reverse-phase, mobile phase = acetonitrile/0.0085M KH_2PO_4 (65:35, v/v, pH 5.0, flow rate of 0.7 ml/min), and detection wavelength = 254 nm.

HPLC Analysis

Sample preparation. Three-milliliter urine (or 1-ml plasma) samples were extracted twice with 5 ml (4 ml for plasma) ethyl acetate, acidified with 0.6 ml (0.2 ml for plasma) 1N HCl followed by additional three ethyl acetate extractions. During each extraction, the samples were shaken at 100 (60 for plasma) OSC/min for 15 min and then stood until phase separation. All five organic extracts were pooled in a clean vial and brought to dryness in a gentle N_2 stream for HPLC analysis. The dried samples were stored at –20°C until HPLC separation.

HPLC separation of PNP and PNP-G in plasma and urine. Separations were performed with a Waters chromatographic system equipped with a 600E solvent delivery system, 717+ autosampler, column temperature control unit, 996 Photodiode Array Detector (PDA), ChemStation with Millennium 2010 software (Waters Corp., Milford, MA), and an automatic fraction collector (Foxy 200, ISCO, Inc., Lincoln, NE). A C_{18} reverse-phase column (μ-Bondapack, 3.9 × 300 mm), operated at 25°C, was eluted with a mobile phase (0.7ml/min) of acetonitrile/0.0085M KH_2PO_4 (65:35, v/v, pH = 5.0). An aliquot of 50 μl of each processed sample was injected to separate PNP and PNP-G to quantify these two compounds via LSC.

HPLC separation methodology was developed using cold standards of PNP and PNP-G in methanol chromatographed and detected at 254 nm. The chromatogram of the nonlabeled standards is shown in Figure 1. The extraction efficiency ranged from 102 to 106% for PNP and 82 to 91%, for PNP-G as calculated by applying a published method (Qiao *et al.*, 1994).

HPLC-LSC analysis. The dried samples were dissolved in methanol (300 μl for urine or 200 μl for plasma), from which 50-μl aliquots were injected for HPLC separation. The peak fractions were automatically collected applying the time windows of 3′30″–5′12″ for PNP-G (peaking at 3.44 min), and 5′12″–6′42″ for PNP (peaking at 5.46 min). Fifteen milliliters of Ecolume™ liquid scintillation cocktail (ICN Biomedicals, Inc., Irvine, CA) was added to each fraction collection, mixed, and stood for at least 4 h before LSC analysis. The fractional amount of compound ***j*** in sample ***i*** assayed by HPLC is

$$\mathrm{DPM}_{j,i} / \sum_{j=1}^{n} \mathrm{DPM}_{j,i} \; (j = 1, \ldots, n).$$

This fraction was multiplied by the total burned DPM in sample ***i*** ($\mathrm{DPM}_{i,\mathrm{burned}}$), and the result was converted to fraction dose of compound ***j*** in sample ***i*** ($A_{j,i}$, % dose):

$$A_{j,i} = \{[(\mathrm{DPM}_{j,i} / \sum_{j=1}^{n} \mathrm{DPM}_{j,i}) \times \mathrm{DPM}_{i,\mathrm{burned}}]/\mathrm{total\ DPM}_{\mathrm{dosed}}\} \times 100\%$$

DPM is disintegrations per minute in the LSC analysis; $n = 2$ refers to the total number of compounds in question (PNP and PNP-G) in the HPLC analysis. The chemical amount-time ($A_{j,i}$-T_i) profiles of PNP and PNP-G in urine and plasma over time and the total ^{14}C amount-time (A_i-T_i) profiles in the ith assay of other samples (termination samples) were used in dTK model formulation.

dTK Modeling and Parameter Estimation

This proposed comprehensive dTK model for topical and iv PNP disposition (Fig. 2) was constructed based on preexisting PNP dermal absorption, metabolism, and modeling data (Chang *et al.*, 1994a; Qiao *et al.*, 1994; Qiao and Riviere, 1995; Williams *et al.*, 1994). Because PNP-G was not identified in perfusate samples from topically dosed isolated perfused porcine skin flap (IPPSF), we excluded a local skin PNP-G compartment in this model, although phase II conjugation reactions (glucuronide and sulfate formation) may occur in pig skin for some other substrates (Qiao *et al.*, 1994; Qiao and Riviere, 1995) or in human skin epidermal cells for PNP (Rugstad and Dybing, 1975). This model has 12 individual compartments (Comps. 1–12) and 3 pooled compartments (Comps. 21–23: dosed tissue pool, central plasma pool, and urine pool, respectively) to predict either the flux of individual chemicals (PNP and PNP-G) or the total radiolabel profiles for comparison with the existing total ^{14}C absorption/disposition data.

To more accurately formulate the dTK model for PNP, we implicitly assumed that the systemic disposition of PNP is independent of application route (topical vs iv), that is, the biologic system handles PNP disposition identically once PNP is introduced into the general circulation, regardless of exposure route. The systemic and excretory parameter estimation was based mainly on the PNP iv bolus data. The topical experiment data were used to estimate the cutaneous (epidermis and above) parameters and also to confirm both the compartmental structure and parameters for the iv model. Model parameters were primarily estimated according to direct analysis of PNP, PNP-G, and total ^{14}C profiles in the central systemic (Comps. 7 and 8) and urinary excretion subunits (Comps. 11 and 12). Observed and calculated plasma profiles were given to facilitate data comparison (this report with other published blood profiles). Liver and other highly perfused organs were not separated from the central systemic (plasma) compartments where the systemic metabolism of PNP occurred. Topical experiments allowed for additional parametric constraints, characterizing local cutaneous disposition by providing some terminal experimental observations of the skin surface (Comp. 1, swab), stratum corneum (Comp. 4, tape strips), and dosing device (DD, Comp. 2,

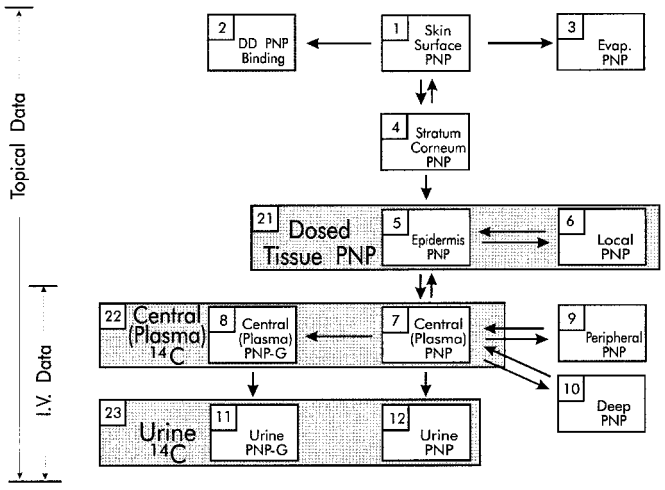

FIG. 2. Comprehensive dermatotoxicokinetic (dTK) model for *p*-nitrophenol (PNP) and *p*-nitrophenyl-β-D-glucuronide (PNP-G) disposition following intravenous and topical exposure *in vivo* in swine (DD = dosing device; Evap. = evaporation)

dosing chamber + wrapping elastic tape + window screening). Nonrecovered ^{14}C was assigned to evaporative loss (Comp. 3) in our topical dTK modeling effort. Because there was no PNP vapor recondensation seen in previous *ex vivo* PNP evaporation and kinetic modeling studies (Brooks and Riviere, 1996; Williams *et al.*, 1994), a one-way connection between compartments 1 (skin surface) and 3 (evaporation) was proposed in this model (Fig. 2). A net PNP transfer from the dosed skin surface (Comp. 1) to dosing device for binding (Comp. 2) was represented by another one-way connection as illustrated. The sum of radiolabel left in the skin compartments (Comps. 4 and 5) below the stratum corneum (the "pool compartment" representing epidermis and other cutaneous tissues, Comp. 21) corresponded to the skin ^{14}C measure.

The 6-compartment iv model (Comps. 7–12) was first formulated by simultaneously fitting the iv urine and plasma $A_{j,i}$-T_i data, employing a numerical least-squares minimization algorithm (KINETICA, North Carolina State University, Raleigh, NC). Both the structure and the mean parameters of the iv model were then fixed (although subject to minor adjustment to best fit the data sets from each individual animals) and incorporated into the 12-compartment topical model (Fig. 2), which was fitted to the topical $A_{j,i}$-T_i and A_i-T_i data from plasma, urine, and other samples assayed. Rate constants, peaks, and peak times were estimated. In the modeling and data simulation, we used fractional dose in each of the anatomical regions or kinetic compartments, as the volumes of many compartments (e.g., dosing device binding–Comp 2; evaporation loss–Comp. 3; and urine–Comps. 11, 12, 23) were not definable/measurable or were extremely variable across individuals. This is the reason for not using concentration profiles, which require a volume term. In fact, we measured concentrations in all the samples and had to convert the concentration results to fractional dose in whole organ/blood by using whole organ weight or volume. For absorption data conversion, the total blood volume (BV, ml/100g) in a pig (< 25 kg) was estimated based on body weight (W, kg) using $BV = 9.5W^{-0.68}$ (Engelhardt, 1966). About 65% (v/v) of the total blood volume was plasma in young pigs, assuming a PCV (packed cell volume) of ~35%. Area under the (zero moment) curve (AUC, % dose × h), area under the first moment curve (AUMC, % dose × h^2), mean residence time (MRT, h), mean absorption time (MAT, h), topical bioavailability (F_{top}, %), $T_{1/2Ka}$ (PNP absorption or PNP-G metabolic formation half-life), $T_{1/2}$ (elimination half-life), distribution volume at steady state (Vss), and clearance (Cl) were calculated according to the following equations (Williams, 1999):

$$AUC = \int_0^\infty f(t)\,dt$$

$$AUMC = \int_0^\infty t \cdot f(t)\,dt$$

$$MRT = AUMC/AUC$$

$$MAT_{top} = MRT_{top} - MRT_{iv} = 1/K_a$$

$$F_{top} = (AUC_{top}/AUC_{iv}) \cdot (Dose_{iv}/Dose_{top}) \cdot 100\%$$

$$T_{1/2Ka} = Ln2 \cdot MAT$$

$$T_{1/2} = Ln2 \cdot MRT$$

$$Vss = Cl \cdot MRT$$

$$Cl = Dose/AUC$$

Data Analysis

Total percutaneous absorption was determined as the percentage of the applied radioactive dose appearing in the urine and feces over the 96-h observation, because no detectable ^{14}C tissue residue was found at the end of experiment (complete excretion). However, total dermal penetration was calculated as the sum of absorption (see above) plus local dosed tissue label residues (Comp. 21 and 4). ANOVA with LSD multicomparison test was conducted wherever applicable at $\alpha = 0.05$ significance level (SAS, Inc., Cary, NC).

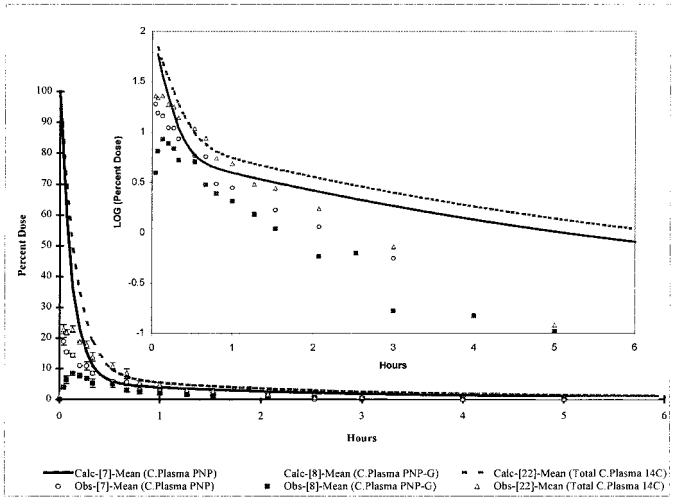

FIG. 3. The observed (symbols) against computer-predicted (lines) mean (± SEM) amount-time profiles of [^{14}C]*p*-nitrophenol (PNP), *p*-nitrophenyl-β-D-glucuronide (PNP-G), and total ^{14}C in the plasma (central compartments 7, 8, and 22) following iv injection of [^{14}C]PNP at a dose of 150 μg in ethanol in female weanling pigs ($n = 4$).

RESULTS

The result of complete HPLC separation of cold PNP standard from its conjugation product of PNP-G is illustrated in Figure 1. Retention times (t_R) for PNP-G and PNP peaks were determined as 3.4 and 5.5 min, respectively. This degree of HPLC separation allowed precise peak fraction collection using programmed time windows for further LSC analysis of the biologic samples with low concentration of ^{14}C radiolabel.

Some key parameters of iv and topical PNP are listed in Tables 1–3. The chemical amount-time profiles of iv and topical PNP are plotted in Figures 3–5 and Figures 6–11, respectively.

In the iv study, total recovery was 99.8% (Table 1). Because this complete recovery was predominately from urine (98.7%), the absolute percutaneous absorption was calculated without any correction/normalization for incomplete recovery or for significant tissue residues after non-occlusive topical application. Only 0.5% of the iv dose was eliminated via the fecal route. Less than 0.04% of the initial iv dose remained in the body by 96 h, indicating no tissue accumulation of PNP or its metabolite in the pig.

With this non-occlusive topical application of PNP, a complete recovery of 97% was determined (Table 1). About 71% of the applied PNP dose was excreted via urinary routes and 0.6% via fecal routes within 96 h (Table 1). Less than 1% of

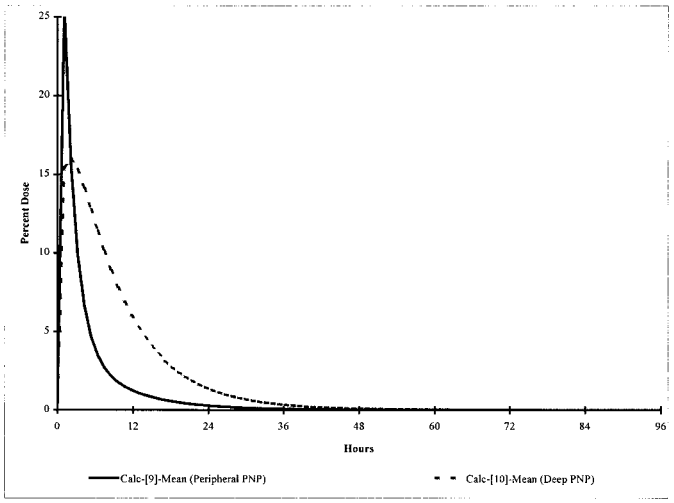

FIG. 4. The dTK model-prediction of [^{14}C]*p*-nitrophenol (PNP) profiles in the peripheral and deep systemic tissues (compartments 9 and 10) following iv injection of [^{14}C]PNP at a dose of 150 μg in ethanol in female weanling pigs ($n = 4$).

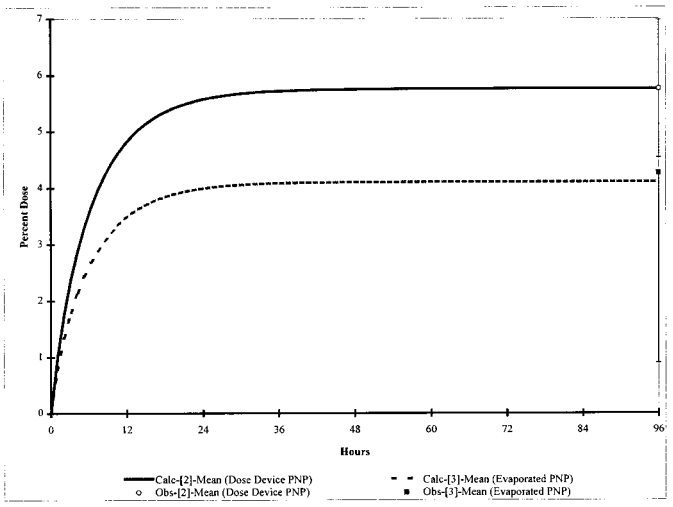

FIG. 6. The observed (symbols) against computer-predicted (lines) mean (± SEM) dosing device binding and evaporative loss profiles of [^{14}C]*p*-nitrophenol (PNP, compartments 2 and 3) following topical exposure of [^{14}C]PNP at a dose of 300 μg in ethanol in female weanling pigs ($n = 4$).

the dose was found in the stratum corneum (SC) layer and 17% remained on the dosed skin surface. Approximately 6% and 2% of the dose were found in the dosing device and in the dosed tissues at 96 h, respectively. PNP did not accumulate in the body after dermal absorption. More label was found in the urine after iv than that following topical [^{14}C]PNP application, although no exposure route effect on fecal excretion was observed (Table 1).

The rate constants of the iv and topical model are given in Table 2. Some key kinetic parameters are also given in Tables 3 and 4. As assumed according to pharmacokinetic theory, most systemic mass transfer rates governing postabsorption processes (distribution, metabolism, and elimination) proved to be identical for topical and iv application ($p > 0.05$), demonstrating route-independent systemic disposition of PNP. Only $k_{7\text{-}12}$ for iv was smaller than that for topical ($p < 0.05$), possibly suggesting the existence of a concentration-dependent or saturable blood-to-urine transfer process. The opposite was found for peripheral tissue PNP returning to blood, that is, a smaller $k_{9\text{-}7}$ was determined with a topical application than with iv. This may indicate that the peripheral tissue compartment for PNP (Comp. 9) is only able to hold a constant amount of PNP.

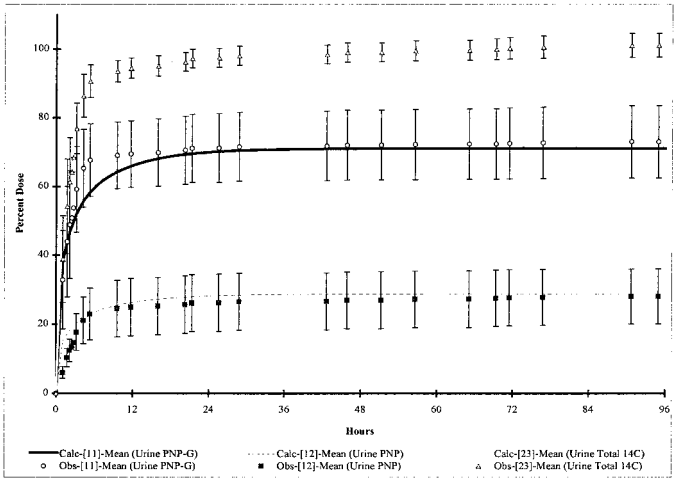

FIG. 5. The observed (symbols) against computer-predicted (lines) mean (± SEM) cumulative urinary excretion profiles of [^{14}C]*p*-nitrophenol (PNP), *p*-nitrophenyl-β-D-glucuronide (PNP-G), and total ^{14}C (compartments 12, 11, and 23) following iv injection of [^{14}C]PNP at a dose of 150 μg in ethanol in female weanling pigs ($n = 4$).

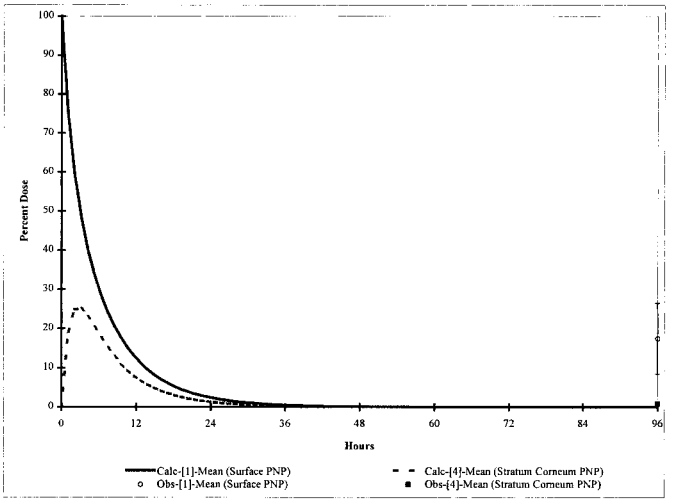

FIG. 7. The observed (symbols) against computer-predicted (lines) mean (± SEM) profiles of [^{14}C]*p*-nitrophenol (PNP)on the dosed skin surface and in the stratum corneum (compartments 1 and 4) following topical exposure of [^{14}C]PNP at a dose of 300 μg in ethanol in female weanling pigs ($n = 4$).

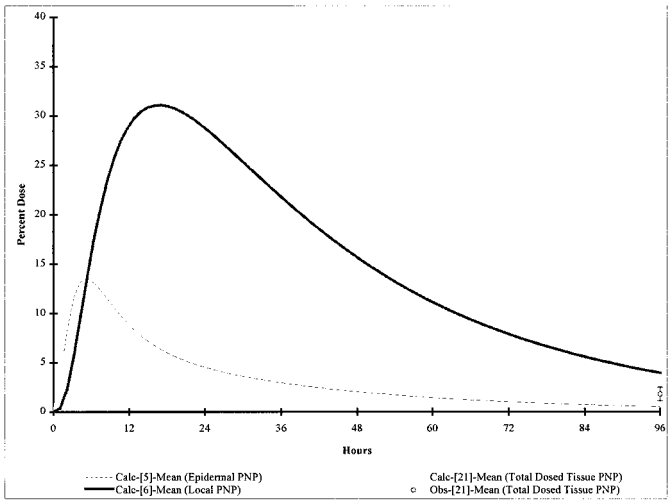

FIG. 8. Mean (± SEM) [^{14}C]*p*-nitrophenol (PNP) profiles in the epidermis (compartment 5) and local cutaneous tissues (compartment 6) and the observed (open circle) against computer-predicted (line) total ^{14}C in the local dosed tissues following topical exposure of [^{14}C]PNP at a dose of 300 μg in ethanol in female weanling pigs (n = 4).

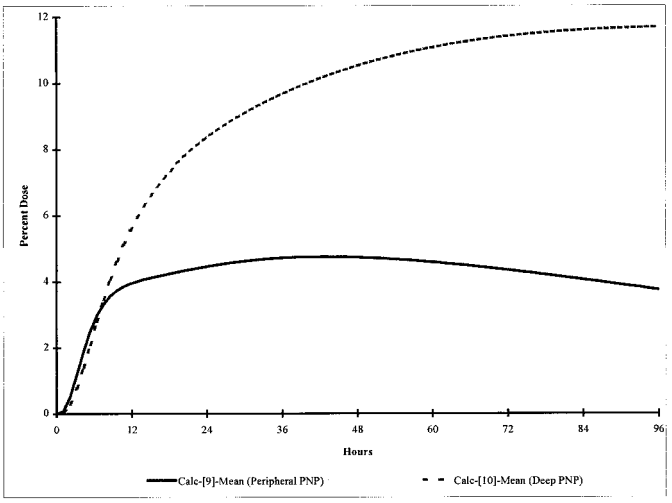

FIG. 10. The dTK model-prediction of [^{14}C]*p*-nitrophenol (PNP) profiles in the peripheral and deep systemic tissues (compartments 9 and 10) following topical exposure of [^{14}C]PNP at a dose of 300 μg in ethanol in female weanling pigs (n = 4).

If more PNP is in the peripheral tissue, as seen with the iv dose, the tissue may not be able to retain the compound and will instead release extra PNP back to the general circulation for systemic elimination. This also explains insignificant PNP tissue accumulation in the pig, as we experimentally observed in this study. Similar AUCs for Comp. 9 were determined for iv and topical exposure, although a larger $k_{9\text{-}7}$ was determined with the iv dose.

MRTs for appropriate compartments after topical dose were generally longer than iv. The model-based calculation of topical PNP bioavailability of 57.4% favorably reflects the observed total dermal absorption of ~70%. Similar results can also be obtained by using AUC ratio ($AUC_{topical}/AUC_{iv}$) either for ^{14}C plasma (56%, Comp. 22) or for PNP in plasma (57%, Comp. 7) (Table 4). No dose adjustment was necessary in the dermal bioavailability calculation, as the AUC unit was the fractional dose-based unit of % dose × h instead of the chemical weight-based unit of μg/ml × h. The dermal absorption half-life of PNP was 18 h, which is similar to the PNP-G

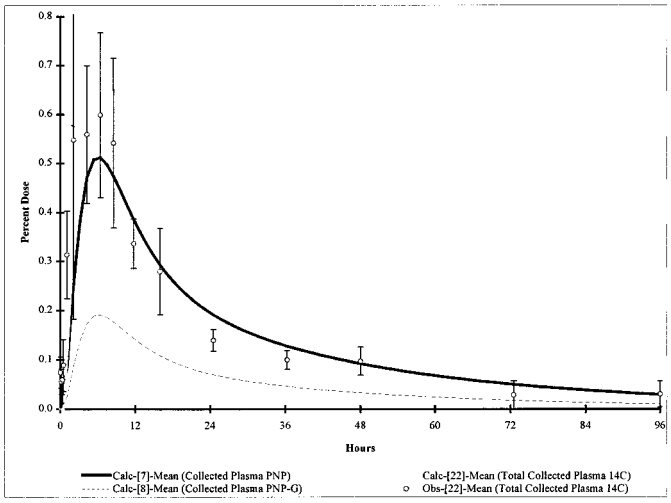

FIG. 9. The observed (open circle) against computer-predicted (lines) mean (± SEM) amount-time profiles of [^{14}C]*p*-nitrophenol (PNP), *p*-nitrophenyl-β-D-glucuronide (PNP-G), and total ^{14}C in the plasma (central compartments 7, 8, and 22) following topical exposure of [^{14}C]PNP at a dose of 300 μg in ethanol in female weanling pigs (n = 4).

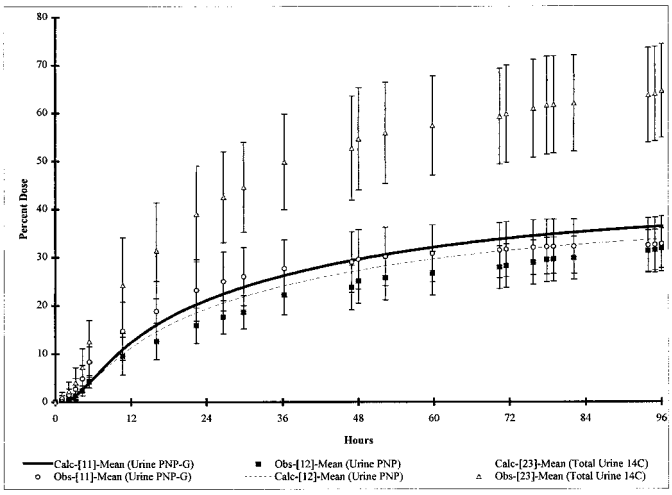

FIG. 11. The observed (symbols) and computer-predicted (lines) mean (± SEM) cumulative urinary excretion profiles of [^{14}C]*p*-nitrophenol (PNP), *p*-nitrophenyl-β-D-glucuronide (PNP-G), and total ^{14}C (compartments 12, 11, and 23) following topical exposure of [^{14}C]PNP at a dose of 300 μg in ethanol in female weanling pigs (n = 4).

TABLE 1

^{14}C Disposition Parameters following Topical (10 μCi, 300 μg/7.5cm^2) and Intravenous (10 μCi, 150 μg) Applications of [^{14}C-Ring-2,6]PNP in Female Weanling Pigs

Compartment	Compartment #	Intravenous (n = 4) (% Dose)	Topical (n = 4) (% Dose)
Dose device	[2]		5.76 (1.22)
Surface swabs	[1]		17.40 (9.01)
SC tape strips	[4]		0.73 (0.18)
Dosed tissue	[5&6] = [21]		1.80 (0.68)
Collected plasma	[7&8] = [22]	0.71 (0.23)[a]	0.02 (0.00)[b]
Total in urine	[11&12] = [23]	98.65 (2.43)[a]	70.92 (9.72)[b]
Total in Feces		0.51 (0.10)[a]	0.55 (0.16)[a]
Unrecovered (evap)	[3]	0.12 (2.41)[a]	2.84 (4.18)[a]
Recovered		99.80 (2.41)[a]	97.17 (4.18)[a]

Note. The data are means ± SEM (n = 4). Significant differences between topical and iv parameters determined by ANOVA-LSD (α = 0.05) are indicated by different superscript letters. PNP, *p*-nitrophenol; SC, stratum corneum; evap, evaporative loss.

metabolic formation half-life ($T_{1/2ka}$ of PNP-G) from PNP conjugation (Table 4). Plasma clearance of PNP was faster than ^{14}C, but not necessarily indicating a slower clearance of PNP-G because the metabolism from PNP to PNP-G occurred in the pooled central compartment of Comp. 22 (Table 4). PNP and ^{14}C elimination half-lives were identical and less than 1 h. Fast distribution half-life was graphically estimated as 5 min (Fig. 3) for PNP, but was slower for pooled ^{14}C. From the computer modeling, we found that equilibrium of dosing device binding and the evaporation processes of PNP were well established around 24 h after dermal exposure (Fig. 6). PNP concentration changes over time on skin surface, in the SC, and dosed tissues were predicted by the model (Figs. 7 and 8). All processes prior to penetration through cutaneous vasculature (absorption) had passed their peaks by the first 24 h after topical application. Plasma and blood profiles of PNP, PNP-G, and total ^{14}C are given in Figure 9. Profiles in the systemic peripheral (Comp. 9) and deep tissue (Comp. 10) compartments are illustrated in Figure 10. As shown in Figure 11, slightly greater than one-half of the total ^{14}C found in urine by 96 h was confirmed to be PNP-G, with the remainder being PNP. More PNP-G was formed in the body during the early stage of the topical experiments.

DISCUSSION

After iv application, plasma PNP profiles (Fig. 3) indicated disposition features for a classical 2- or 3-compartment TK model as seen in a semilogarithmic drug amount-time plot. The distribution half-lives are about 5 min for PNP but 6–7 min for total label. Elimination half-lives of PNP and ^{14}C label were about 50 min (Fig. 3 and Table 4). Approximately 95% of the radioactive PNP dose was eliminated from blood within 1 h after iv application. This plot also revealed that PNP contributed much more to total plasma ^{14}C counts than PNP-G during the first 30–60 min. Parallel decline of PNP and PNP-G profiles in plasma was determined thereafter (Fig. 3). Intravenous PNP disposition kinetics reported here were very similar to those of parathion previously determined after iv application in the pig (Qiao *et al.*, 1994).

Computer simulation of the PNP residue profiles over time in the systemic tissue compartments (Fig. 4) is useful in estimating overall body burden and time for maximal tissue exposure of PNP. For example, we can predict that by 1–1.5 days post PNP iv application, all the tissues/organs of the animals will be cleared of PNP. This was verified by the fact that urine excretion of label was completed by about 1 day (Fig. 5) and by complete recovery of the iv PNP dose (Table 1). The highest modeled tissue concentration was observed around 2–3 h after iv dose. Accordingly, the highest possibility of tissue toxicity could be expected during this time frame. For the shallow tissue compartment (Comp. 9, relatively quicker equilibration with blood), a peak time was determined at about 2 h, while a deeper tissue compartment (Comp. 10, relatively slower equilibration with blood) may hold the largest PNP burden at 3 h (Fig. 4). This provides useful information for PNP tissue kinetics study design and drug residue prediction in tissues.

The urine excretion of the iv PNP and its conjugate PNP-G could be completed by about 1 day, and more than 90% of the iv dose was excreted in urine within the first 12 h (Fig. 5). PNP-G and PNP contribute about two-thirds and one-third of the total urine label, respectively (Fig. 5). This was consistent with the time frame of modeled tissue residue profiles (Fig. 4). Very similar results were obtained with urine PNP excretion

TABLE 2

PNP Pharmacokinetic Modeling Parameters (h^{-1}, mean ± SEM) following Topical (10 μCi, 300 μg/7.5cm^2) and Intravenous (10 μCi, 150 μg) Applications of [^{14}C-Ring-2,6]PNP in Female Weanling Pigs

Rates	Intravenous (n = 4)	Topical (n = 4)		
$k_{7\text{-}9}$	3.350 (0.065)[a]	3.500 (0.314)[a]	$K_{1\text{-}2}$	0.011 (0.002)
$k_{9\text{-}7}$	0.963 (0.021)[a]	0.479 (0.156)[b]	$K_{1\text{-}3}$	0.009 (0.007)
$k_{7\text{-}10}$	1.075 (0.048)[a]	2.023 (0.766)[a]	$K_{1\text{-}4}$	0.270 (0.052)
$k_{10\text{-}7}$	0.183 (0.011)[a]	0.083 (0.045)[a]	$K_{4\text{-}1}$	0.165 (0.024)
$k_{7\text{-}12}$	0.890 (0.243)[b]	2.475 (0.085)[a]	$K_{4\text{-}5}$	0.373 (0.043)
$k_{7\text{-}8}$	2.483 (0.557)[a]	2.638 (0.090)[a]	$K_{5\text{-}6}$	0.358 (0.036)
$k_{8\text{-}11}$	6.725 (0.613)[a]	7.425 (0.246)[a]	$K_{6\text{-}5}$	0.075 (0.009)
			$K_{5\text{-}7}$	0.283 (0.044)
			$K_{7\text{-}5}$	0.070 (0.006)

Note. The data are means ± SEM (n = 4). Significant differences between topical and iv parameters determined by ANOVA-LSD (α = 0.05) are indicated by different superscript letters. PNP, *p*-nitrophenol; K***i-j***, chemical transfer rate constant from compartment ***i*** to compartment ***j***.

TABLE 3
PNP Disposition Kinetic Parameters (mean ± SEM) following Topical (10 μCi, 300 μg/7.5cm^2) and Intravenous (10 μCi, 150 μg) Applications of [^{14}C-Ring-2,6]PNP in Female Weanling Pigs

		AUC (% dose × h)		MRT (h)	
Compartment	Comp. #	Intravenous (n = 4)	Topical (n = 4)	Intravenous (n = 4)	Topical (n = 4)
Surface swabs	[1]		528.21 (97.45)		6.26 (0.86)
Dose device	[2]		NA		51.42 (0.39)
Evaporation	[3]		NA		51.42 (0.39)
SC tape strips	[4]		258.57 (26.83)		7.79 (0.97)
Epidermis	[5]		324.56 (36.23)		24.65 (2.27)
Local tissue	[6]		1474.92 (116.80)		36.12 (1.16)
Dosed tissue ^{14}C	[21]		1799.48 (150.30)		34.08 (1.34)
Plasma PNP	[7]	24.02 (2.34)[a]	13.69 (2.06)[a]	1.21 (0.07)[b]	28.25 (2.70)[a]
Plasma PNP-G	[8]	9.11 (1.15)[a]	4.98 (0.99)[a]	1.24 (0.08)[b]	28.39 (2.69)[a]
Collected plasma ^{14}C	[22]	33.13 (2.10)[a]	18.68 (3.04)[a]	1.21 (0.07)[b]	28.29 (2.70)[a]
Peripheral PNP	[9]	103.90 (15.84)[a]	394.83 (316.50)[a]	4.24 (0.53)[b]	34.83 (6.91)[a]
Deep PNP	[10]	188.67 (32.80)[a]	878.59 (480.00)[a]	8.57 (0.87)[b]	44.28 (7.85)[a]
Urine PNP-G	[11]	NA	NA	49.98 (0.22)[b]	59.16 (0.91)[a]
Urine PNP	[12]	NA	NA	49.93 (0.21)[b]	59.10 (0.91)[a]
Total urine ^{14}C	[23]	NA	NA	49.96 (0.21)[b]	59.13 (0.91)[a]

Note. The data are means ± SEM (n = 4). Significant differences between topical and iv parameters determined by ANOVA-LSD (α = 0.05) are indicated by different superscript letters. PNP, *p*-nitrophenol; PNP-G, *p*-nitrophenyl-β-D-glucuronide; SC, stratum corneum; AUC, area under the curve; MRT, mean residence time (see details in *Materials and Methods*); NA, not applicable.

following iv dose of its parent compound parathion (Qiao *et al.*, 1994). Therefore, urine PNP monitoring can serve as an easy and reliable tool to assess the exposure and resultant tissue residue of PNP and likely its parent compound (parathion) exposure in the pig model. Obviously, this study supports the strategic development of risk assessment by ATSDR using urine PNP as a biomarker of methyl parathion exposure due to the illegal house spraying with this pesticide in the United States (ATSDR, 1996). However, this biomonitoring is appropriate only if methyl parathion shows a quick and complete biotransformation to PNP in the human. Otherwise, PNP urine level monitoring may not be able to serve as an ideal tool for methyl parathion risk assessment if the disposition processes of methyl parathion or its active metabolite methyl paraoxon are largely different from that of PNP. A much faster urine excretion rate was determined for PNP-G than for PNP, as a 3–7 times faster blood-to-urine chemical transfer rate of PNP-G ($k_{8\text{-}11}$) than PNP ($k_{7\text{-}12}$) was predicted (Table 2). Similar rate ratio (~2) and absolute values of PNP-G (5.01 h^{-1}) and PNP (3.19 h^{-1}) blood-to-urine transfer rates were also determined after parathion exposure (Qiao *et al.*, 1994). This is consistent with the principle of chemical detoxification in the body and the fact that PNP-G is more water soluble and therefore more readily excreted via the renal route.

TABLE 4
PNP Disposition Kinetic Parameters Derived from Plasma Data Topical (10 μCi, 300 μg/7.5cm2) and Intravenous (10 μCi, 150 μg) Applications of [^{14}C-Ring-2,6]PNP in Female Weanling Pigs

	[7] PNP	[8] PNP-G	[22] Total ^{14}C
Topical			
F_{top} (%)	57.01	NA	56.37
MAT_{top} (h)	27.05	27.15	27.07
K_a (h^{-1})	0.037	0.037	0.037
$T_{1/2Ka}$ (h)	18.75	18.82	18.77
Intravenous			
C_{lp} (ml/h/kg)	233.16	NA	169.02
V_{ss} (ml/kg)	5.02	NA	3.66
$T_{1/2}$ (h)	0.84	0.86	0.84

Note. PNP, *p*-nitrophenol; F_{top}, topical bioavailability; MAT_{top}, mean absorption time for topical dose; K_a, PNP absorption or PNP-G metabolic formation rate constant; $T_{1/2Ka}$, half-life for absorption/metabolic formation; C_{lp}, plasma clearance; V_{ss}, distribution volume at steady state; $T_{1/2}$, elimination half-life.

As shown in Figure 6, dosing device PNP binding was expressed as the net transfer of PNP from the topical dose (vapor, liquid, or solid) to the dosing device and occurred only during the first 24 h. The binding was saturated or a zero net transfer between the dose and the device was reached at 24 h. Dose evaporation only happened during the first 24 h after exposure (Fig. 6) with evaporation rate constant of 0.009 h^{-1} (Table 2) under non-occlusive conditions. Very low *in vivo* PNP evaporation loss of 3% was estimated using the dose-recovery difference approach (Qiao *et al*, 1994, Qiao and Riviere, 1995) in this study.

It seems that this dTK model could underestimate the skin surface residue profile, as a much higher surface residue was

experimentally determined when compared to the computer simulation at the end of the experiments (Fig. 7). This may be due partially to the back-and-forth direct contact of the skin surface against the contaminated dosing chamber. It is possible to reload some ^{14}C-PNP to the surface from the dosing device right before the termination of the experiments. This would surely make an unreasonably higher assayed surface ^{14}C residue than the computer simulation result. In addition, math modeling limitations (e.g., use of simplest model, more weight for more important or more reliable sample data sets, etc.) may also contribute to this and other differences between the observed and calculated results, although effort was made to get the best overall data fitness.

Theoretically, postabsorption disposition kinetics (i.e., distribution, metabolism, and excretion) of a drug should be intrinsic and route independent. Therefore, most dTK model parameters (transfer rates) governing postabsorption processes should be similar for a compound either directly dosed via various exposure routes (topical, oral, inhalation, iv, etc.) or metabolically generated in the skin during penetration. Only some mass transfer rates, especially the absorption/metabolic formations rates, may be affected by the compound dosed (PNP dosed directly or a dose of its parent compound such as parathion or methyl parathion) or by the dosing method. This study demonstrated that PNP local tissue distribution, PNP metabolism to PNP-G, and PNP blood-to-urine transfer rates were similar for both directly-dosed PNP, as reported in this work, and for parathion-derived PNP, as in our previous study in the pig (Qiao *et al*., 1994). The results presented here demonstrate that the model rate constants with an identical dTK model structure were similar for iv and topical PNP application (Table 2). Therefore, via this study it was suggested that in complex *in vivo* dTK modeling, toxicants should be intravenously dosed and the iv data were modeled initially to simplify the more complex topical modeling task.PNP absorption has been demonstrated to be as significant as 6–22% within 8 h after *in vitro, ex vivo*, or *in vivo* dermal exposure in pig models in a dose-dependent fashion (Brooks and Riviere, 1996; Chang *et al.,* 1994a; Qiao *et al.,* 1996). Similarly, other researchers reported 35% and 11% of topical PNP could be absorbed in rabbits and dogs, respectively (ATSDR, 1996). If the experiment was extended to 4 days as with this *in vivo* pig model, over 70% of the topical PNP dose could be absorbed. Tissue residues were also found to be insignificant (ATSDR, 1996; Qiao *et al.,* 1996). PNP dermal absorption has also been studied in other *in vitro* static and flow-though diffusion cell systems with animal or human skin (Hinz *et al.*, 1991; Hotchkiss *et al.,* 1992). PNP absorption after oral and inhalation exposure was found to be complete and quick. More than 80–90% of an oral PNP dose was absorbed in rabbits, and the blood T_{max} was only several minutes in monkeys (ATSDR, 1996).

Quite often, the absolute amount (mass) of dermally absorbed penetrant can be increased with dose, although the fractional dose absorbed may be decreased. Interestingly, 2- to 4-fold increases in fractional PNP dermal absorption were observed with dose increases from 4 to 400 μg PNP/cm^2 in our *in vitro* (Chang *et al.,* 1994a) and *ex vivo* IPPSF (Brooks and Riviere, 1996) dermal absorption studies. Additionally, larger PNP doses also gave a quicker absorption peak (T_{max}), deeper skin penetration, and a larger local tissue residue in our *ex vivo* study (Brooks and Riviere, 1996). This suggests that PNP enhances its own dermal absorption in terms of both rate and extent. PNP also enhances dermal absorption of its parent compound parathion (Chang *et al*., 1994a).

Conjugation, especially with glucuronide, is the major PNP metabolic pathway in animals. PNP glucuronidation proceeded in kidney, lung, and liver, but sulfation occurred almost exclusively in liver (Machida *et al.,* 1982). It was demonstrated that human skin epithelial cells have PNP conjugation activity (Rugstad and Dybing, 1975). PNP was rapidly conjugated up to 70% of an ip dose by 3 h and up to 95% by 12 h, and PNP-G was the dominant metabolite completely excreted in urine (Gessner, 1974). It was demonstrated that PNP-G accounted for 70% of the oral PNP dose in rabbits. Similar results were obtained from a rat study after PNP iv dose, with a very quick formation of PNP conjugation products within 1 min (Machida *et al.,* 1982). This demonstrated that PNP-G also accounted for two-thirds of the total excretion in the pig (Fig. 5), which is similar to PNP metabolic disposition in other species via different application routes. PNP conjugation is not sex specific but may be saturable/dose-dependent. PNP conjugation reactions seemed to be limited by the hepatic blood perfusion rate, i.e., the hepatic extraction ratio of PNP can be as high as 1.0 (Machida *et al.,* 1982). It was also found that extrahepatic conjugation metabolism of PNP was considerable (46% of the entire glucuronidation capacity) in animals (Machida *et al*., 1982). At least three isoenzymes are responsible for PNP conjugation in the rat (Antoine *et al*., 1993). Up to 1992, no study was conducted regarding excretion in humans following dermal exposure (ATSDR, 1992).

About 78% of the absorbed PNP dermal dose in the rabbit and 92% of an iv dose in the dog appeared in the urine within 1 day. Fecal elimination is very minor ($<$ 1%) in both cases (ATSDR, 1996). In this pig study, urine excretion of PNP (one-third) and PNP-G (two-thirds) was completed within 1 day after iv application of PNP (Fig. 5). However, a continuous urine excretion was observed following dermal exposure. This was due mainly to the prolonged dermal exposure (no skin wash during the 4-day study) and continuous percutaneous absorption (Fig. 11) but not due to PNP/PNP-G release from tissues; label excretion is fast and tissue residue is insignificant after both iv and topical exposure of PNP. PNP-G is more polar than the parent PNP and thus easier to excrete via the renal route. Similar to the dog, rabbit (ATSDR, 1996), and rat (Gessner, 1974) studies, we found that fecal excretion was very minor ($\sim$0.5%) following both iv and dermal exposure of PNP in the pig (Table 1).

Urinary PNP, as a sole biomarker of human pesticide exposure, was used as a key decision-making criterion for a remediation strategy related to the illegal indoor application of methyl parathion in several states in the United States (ATSDR, 1996; Grissom *et al*., 1998). Urine PNP can be from sources other than methyl parathion exposure such as direct PNP exposure from methyl parathion environmental degradation, although methyl parathion imposes the major health concern via its active metabolite of methyl paraoxon. Additionally, PNP can greatly enhance dermal absorption of compounds like parathion and itself (Chang *et al*., 1994a,b). Due to all of those, the urine PNP monitoring strategy for methyl parathion dermal risk assessment should be carefully implemented. When aged methyl parathion containing PNP (e.g., methyl parathion degradation) is exposed to skin, the resultant urine PNP should represent two sources—direct dermal absorption of PNP and metabolic generation of PNP from systemic/cutaneous metabolism of methyl parathion. Therefore, environmental methyl parathion levels and urinary PNP levels alone might not be adequate for assessing human health threats associated with indoor methyl parathion exposure. A more integrated exposure assessment strategy, based on the better understanding of mixed exposure and more importantly metabolic and environmental degradation kinetics of methyl parathion, becomes essential for risk analysis and management of the methyl parathion house spray incident.

In conclusion, the PNP TK modeling strategy developed here will be useful in the comprehensive dTK modeling of its parent compounds for human dermal risk assessment as well as in transdermal drug delivery studies. PNP postabsorption disposition kinetics were exposure independent. This model is structurally identical to the model used for published parathion modeling work. PNP was one of the most effective percutaneous penetrants, with percutaneous absorption of over 70% after dermal exposure in swine. PNP and its conjugation metabolite PNP-G were rapidly and completely transported from blood into urine with very minor fecal excretion and insignificant tissue residues in swine. Urinary excretion is the primary elimination route for PNP and its metabolite, with about one-third as PNP and two-thirds as PNP-G after iv, but equally as PNP and PNP-G following topical PNP exposure. The results support the strategy of applying urine PNP as a biomarker of OP pesticide exposure assessment, although some precautions have to be taken.

ACKNOWLEDGMENTS

This work was supported mainly by NCSU/CCTRP funds. The authors thank Drs. N. A. Monteiro-Riviere in NCSU, S. C. Soderholm, F. H. Frasch in NIOSH, and P. L. Williams at Polytheoretics, Inc. for their assistance in the preparation of this manuscript.

REFERENCES

Antoine, B., Boutin, J. A., and Siest, G. (1993). Heterogeneity of hepatic UDP-glucuronosyltransferase activities: investigations of isoenzymes involved in p-nitrophenol glucuronidation. *Comp. Biochem. Physiol. C.* **106,** 241–248.

ATSDR (1992). Toxicological Profile for Nitrophenols: 2-Nitrophenol, 4-Nitrophenol. US DHHS, PHS, Agency for Toxic Substance and Disease Registry (ATSDR), Atlanta, GA.

ATSDR (1996). Public health Advisory for methyl parathion/Pascagoula, Jackson County, Mississippi, US DHHS, PHS, ATSDR, AHAC, Atlanta, GA, Dec. 3.

Bartek, M. J., Labudde, J. A., and Maibach, H. I. (1972). Skin permeability *in vivo*: comparison in rat, rabbit, pig and man. *J. Invest. Dermatol.* **58**, 114–123.

Berry, C., Stellon, A., and Hallinan, T. (1975). Guinea pig liver microsomal UDP-glucuronyltransferase: compartmented or phospholipid-constrained? *Biochim. Biophys. Acta.* **403,** 335–344.

Bock, K. W., Frohling, W., Remmer, H., and Rexer, B. (1973). Effects of phenobarbital and 3-methylcholanthrene on substrate specificity of rat liver microsomal UDP-glucuronyltransferase. *Biochim. Biophys. Acta.* **327,** 46–56.

Brooks, J. D., and Riviere, J. E. (1996). Quantitative percutaneous absorption and cutaneous distribution of binary mixtures of phenol and para-nitrophenol in isolated perfused porcine skin. *Fundam. Appl. Toxicol*. **32,** 233–243.

Chang, S. K., Dauterman, W. C., and Riviere, J. E. (1994a). Percutaneous Absorption of Parathion and Its Metabolites Paraoxon and P-Nitrophenol Administered Alone or In Combination: *In vitro* Flow Through Diffusion Cell System. *Pest Biochem. Physiol.* **48,** 56–62.

Chang, S. K., Williams, P. L., Dauterman, W. C., and Riviere, J. E. (1994b). Percutaneous absorption, dermatopharmacokinetics and related bio-transformation studies of carbaryl, lindane, malathion, and parathion in isolated perfused porcine skin. *Toxicology* **91,** 269–280.

Cooper, A. R., Overholt, L., Tillquist, H., Jamison, D. (1997). 4-Nitrophenol. In *Cooper's Toxic Exposures* (A. R. Cooper, L. Overholt, H. Tillquest, and D. Jamison, Eds.), pp. 1610–1619. CRC Press, Inc., New York, NY.

Engelhardt, W. V. (1966). Swine cardiovascular physiology- a review. In *Swine in Biomedical Research* (L. K. Bustad and R. McClellan, Eds.), pp. 307–329. Frayn Printing Co., Seattle, WA.

Gessner, T. (1974). Studies of glucuronidation and sulfation in tumor-bearing rats. *Biochem. Pharmacol.* **23,** 1809–1816.

Grissom, R. E., Akin, E., Susten, A. S., Brackin, B., and Stilman, T. (1998). Residential exposure to methyl parathion (MP). *Toxicol. Sci.* **42 (1s),** 44.

Hamada, N., and Gessner, T. (1975). Effect of 3-methylcholanthrene pretreatment on glucuronidation and sulfation in perfused rat liver. *Drug Metab. Dispos.* **3,** 407–416.

Hawkins, G. S. Jr., and Reifenrath, W. G. (1984). Development of an *in vitro* model for determining the fate of chemicals applied to skin. *Fundam. Appl. Toxicol.* **4**, S133–S144.

Hinz, R. S., Lorence, C. R., Hodson, C. D., Hansch, C., Hall, L. L., and Guy, R. H. (1991). Percutaneous penetration of para-substituted phenols *in vitro*. *Fundam. Appl. Toxicol.* **17,** 575–583.

Honeycutt, R. C., Zweig, G., and Ragsdale, N. N. (1985). *Dermal exposure related to pesticide use.* American Chemical Society, Washington, DC.

Hotchkiss, S. A., Hewitt, P., Caldwell, J., Chen, W. L., and Rowe, R. R. (1992). Percutaneous absorption of nicotinic acid, phenol, benzoic acid and triclopyr butoxyethyl ester through rat and human skin *in vitro*: further validation of an *in vitro* model by comparison with *in vivo* data. *Food Chem. Toxicol.* **30,** 891–899.

Kutz, F. W., Cook, B. T., Carter-Pokras, O. D., Brody, D., and Murphy, R. S. (1992). Selected pesticide residues and metabolites in urine from a survey of the U.S. general population. *J. Toxicol. Environ. Health* **37**, 277–291.

Machida, M., Morita, Y., Hayashi, M., and Awazu, S. (1982). Pharmacokinetic

evidence for the occurrence of extrahepatic conjugative metabolism of p-nitrophenol in rats. *Biochem. Pharmacol.* **31,** 787–791.

Meyer, W., Schwarz, R., and Neurand, K. (1978). The skin of domestic animals as a model for the human skin, with special reference to the domestic pig. In *Current Problems in Dermatology*. Vol.7 (G. S. Simon *et al.*, Eds.), pp. 39–52. Karger, Basel, Switzerland.

Minck, K., Schupp, R.R., Illing, H. P., Kahl, G. F., and Netter, K. J. (1973). Interrelationship between demethylation of p-nitroanisole and conjugation of p-nitrophenol in rat liver. *Naunyn- Schmiedebergs Arch. Pharmacol.* **279,** 347–360.

Moldeus, P., Vadi, H., and Berggren, M. (1976). Oxidative and conjugative metabolism of p-nitroanisole and p-nitrophenol in isolated rat liver cells. *Acta Pharmacol. Toxicol. (Copenh.).* **39,** 17–32.

Monteiro-Riviere, N. A., and Riviere, J. E. (1996). The pig as a model for cutaneous pharmacology and toxicology. In *Advances in Swine in Biomedical Research* (M. E. Tumbleson and L. Schook, Eds.). pp. 425–458. Plenum Press, New York.

Pena-Egido, M. J., Marino-Hernandez, E. L. Santos-Buelga, C., and Rivas-Gonzalo, J. C. (1988). Urinary excretion kinetics of *p*-nitrophenol following oral administration of parathion in the rabbit. *Arch. Toxicol.* **62**, 351–354.

Qiao, G. L., Brooks, J. D., and Riviere, J. E. (1997). Pentachlorophenol dermal absorption and disposition from soil in swine: effects of occlusion and skin microorganism inhibition. *Toxicol. Appl. Pharmacol.* **147,** 234–246.

Qiao, G. L., Chang, S. K., Brooks, J. D., and Riviere, J. E. (1996), Pharmacokinetic modeling of p-nitrophenol and its conjugation metabolite in swine. *Pharm. Res.* **13,** S417.

Qiao, G. L., Chang, S. K., and Riviere, J. E. (1993). Effects of anatomical site and occlusion on the percutaneous absorption and residue pattern of 2,6-[ring-^{14}C]parathion *in vivo* in pigs. *Toxicol. Appl. Pharmacol.* **122**, 131–138.

Qiao, G. L., and Riviere, J. E. (1995). Significant effects of application site and occlusion on the pharmacokinetics of cutaneous penetration and biotransformation of parathion *in vivo* in swine. *J. Pharm. Sci* **84**, 425–432.

Qiao, G. L., Williams, P. L., and Riviere, J. E. (1994). Percutaneous absorption, biotransformation and systemic disposition of parathion *in vivo* in swine. I. Comprehensive pharmacokinetic model. *Drug Metab. Dispos.* **23,** 459–471.

Reifenrath, W. G., Chellquist, E. M., Shipwash, E. A., Jederberg, W. W., and Krueger, G. G. (1984). Percutaneous penetration in the hairless dog, weanling pig and grafted athymic nude mouse: evaluation of models for predicating skin penetration in man. *Br. J. Dermatol.* **3** (S27), 123–135.

Reifenrath, W. G. and Hawkins, G. S. (1986). The weanling Yorkshire pig as an animal model for measuring percutaneous penetration. In *Swine in Biomedical Research* (M. E. Tumbelson, Ed.). pp. 673–680. Plenum Press, New York.

Rugstad, H. E., and Dybing, E. (1975). Glucuronidation in cultures of human skin epithelial cells. *Eur. J. Clin. Invest.* **5,** 133–137.

Vessey, D. A., Goldenberg, J., and Zakim, D. (1973). Differentiation of homologous forms of hepatic microsomal UDP-glucuronyltransferase. II. Characterization of the bilirubin conjugating form. *Biochim. Biophys. Acta* **309,** 75–82.

Vessey, D. A., and Zakim, D. (1973).The identification of a unique p-nitrophenol conjugating enzyme in guinea pig liver microsomes. *Biochim. Biophys. Acta* **315,** 43–48.

Wang, R. G. M., Franklin, C. A., Honeycutt, R. C., and Reinert, J. C. (1989). Biological monitoring for pesticide exposure. American Chemical Society, Washington, DC.

Wester, R. C., and Maibach, H. I. (1989). *Percutaneous absorption and inherent toxicity. Biological monitoring for pesticide exposure.* pp. 131–136. American Chemical Society, Washington, DC.

Wester, R. C., Melendres, J., Sedik, L., Maibach, H. I., and Riviere, J. E. (1998). Percutaneous absorption of salicylic acid, theophylline, 2,4-dimethylamine, diethyl hexyl phthalate acid and p-aminobenzoic acid in the isolated perfused porcine skin flap compared to man *in vivo*. *Toxicol. Appl. Pharmacol.* **151,** 159–165.

Williams, P. L. (1999). Noncompartmental models. In *Comparative Pharmacokinetics: Principles, Techniques, and Applications* (J. E. Riviere, Ed.). pp. 148–167. ISU Press, Ames, Iowa.

Williams, P. L, Brooks, J. D., Inman, A. O., Monteiro-Riviere, N. A., and Riviere, J. E. (1994). Determination of physicochemical properties of phenol, p-nitrophenol, acetone and ethanol relevant to quantitating their percutaneous absorption in porcine skin. *Res. Commun. Chem. Pathol. Pharmacol.* **83,** 61–75.